Computer Methods and Programs in Biomedicine 255 (2024) 108325

Contents lists available at ScienceDirect

Computer Methods and Programs in Biomedicine

journal homepage: www.sciencedirect.com/journal/computer-methods-and-programs-in-biomedicine

# Influence of the pressure wire on the fractional flow reserve calculation: CFD analysis of an ideal vessel and clinical patients with stenosis

Alberto Otero-Cacho [a,e,f,*], Manuel Insúa Villa [a], Diego López-Otero [b,c], Brais Díaz-Fernández [b,c], María Bastos-Fernández [b,c], Vicente Pérez-Muñuzuri [d,f], Alberto P. Muñuzuri [e,f], José Ramón González-Juanatey [b,c]

[a] FlowReserve Labs S.L., Santiago de Compostela, Spain
[b] Cardiology and Intensive Cardiac Care Department, University Hospital of Santiago de Compostela, Santiago de Compostela, Spain
[c] Centro de Investigación Biomédica en Red de Enfermedades Cardiovasculares (CIBERCV), Madrid, Spain
[d] CRETUS Research Center, University of Santiago de Compostela, Spain
[e] Galician Center for Mathematical Research and Technology (CITMAga), Santiago de Compostela, E15782, Spain
[f] Group of Nonlinear Physics, Department of Physics, University of Santiago de Compostela, Santiago de Compostela, E15782, Spain

A R T I C L E I N F O

*Keywords:*
Stenosis
Fractional flow reserve
CFD modeling
Pressure wire
Computed tomography

A B S T R A C T

*Background and objective:* Fractional Flow Reserve (FFR) is generally considered the gold standard in hemodynamics to assess the impact of a stenosis on the blood flow. The standard procedure to measure involves the displacement of a pressure guide along the circulatory system until it is placed next to the lesion to be analyzed. The main objective of the present study is to analyze the influence of the pressure guide on the invasive FFR measurements and its implications in clinical practice.

*Methods:* We studied the influence of pressure wires on the measurement of Fractional Flow Reserve (FFR) through a combination of Computational Fluid Dynamics (CFD) simulations using 45 clinical patient data with 58 lesions and ideal geometries. The analysis is conducted considering patients that were subjected to a computer tomography and also have direct measurements using a pressure guide. Influence of the stenosis severity, degree of occlusion and blood viscosity has also been studied.

*Results:* The influence of pressure wires specifically affects severe stenosis with a lumen diameter reduction of 50 % or greater. This type of stenosis leads to reduced hyperemic flow and increased coronary pressure drop. Thus, we identified that the placement of wires during FFR measurements results in partial obstruction of the coronary artery lumen, leading to increased pressure drop and subsequent reduction in blood flow. The severity of low FFR values associated with severe stenosis may be prone to overestimation when compared to stenosis without severe narrowing. These results have practical implications, particularly in the interpretation of lesions falling within the "gray zone" (0,75−0,80).

*Conclusions:* The pressure wire's presence significantly alters the flow on severe lesions, which has an impact on the FFR calculation. In contrast, the impact of the pressure wire appears to be reduced when the FFR is larger than 0.8. The findings provide critical information for physicians, emphasizing the need for cautious interpretation of FFR values, particularly in severe stenosis. It also offers insights into improving the correlation between FFRct models and invasive measurements by incorporating the influence of pressure wires.

## 1. Introduction

Myocardial infarction (MI) and sudden cardiac death (SCD) are the leading cause of mortality worldwide [1]. By 2030, the mortality number is expected to grow to more than 23.6 million, and a very large portion is attributed to atherosclerosis [2]. Atherosclerosis is a chronic and systemic inflammatory disease of the arterial vessels characterized by the formation of coronary stenosis (atherosclerotic plaques) in the vasculature [3] Stenosis produces a reduction in arterial diameter, restricting blood flow, which can cause ischemia [4]. There are a multitude of diagnostic tests that help physicians to evaluate stenosis, including chest X-ray, echocardiography, electrocardiogram, and

* Corresponding author.
*E-mail address:* alberto.otero.cacho@usc.es (A. Otero-Cacho).

https://doi.org/10.1016/j.cmpb.2024.108325
Received 3 February 2024; Received in revised form 7 July 2024; Accepted 11 July 2024
Available online 14 July 2024

cardiac catheterization. The latter quantifies the reduction in blood flow through a pressure ratio known as fractional flow reserve (FFR) [5]. FFR is a diagnostic test used to quantify the severity of coronary artery stenosis [6,7].

In the past, the severity of coronary stenosis was defined in terms of resistance, geometry, pressure gradient or coronary flow reserve because the relationship between pressure and flow is not direct. However, Pijls et al. [8] demonstrated that, under conditions of maximum hyperemia, there is a linear relationship between cardiac output and pressure gradient. This relationship is expressed in terms of the FFR, which is nowadays the gold standard to determine the severity of coronary stenosis [9,10]. The FAME I/II [11,12] studies were published in 2009–2010 and concluded that routine FFR measurements in patients with multivessel coronary artery disease undergoing PCI (percutaneous coronary intervention) significantly reduces mortality and myocardial infarction compared to angiographically guided PCI. Previous studies [13–15] showed by the first time the diagnostic capability of a new method for noninvasive measurement of fractional flow reserve derived from Computed Tomography Angiography, FFRct.

FFRct is based on computational simulation of fluid dynamics (CFD) inside the arteries [16,17]. A 3D coronary model is reconstructed from the images of computed tomography angiography that is used by the CFD to simulate the flow. One of the main advantages of FFRct is that it is a noninvasive technique that provides a complete map of the FFR index in the entire coronary tree [16,18–20] unlike the invasive method where the value is only obtained in the area where it is measured. In addition, it offers the possibility of measuring other parameters such as the wall shear stress (WSS), hyperemic stenosis resistance (HSR), etc. [21–25].

In the invasive test, the pressure wire alters the FFR measurement [13] as introduces an uncertainty that strongly depends on the type of lesion. The pressure wire in the presence of a stenosis shows a nonlinear response to the reduction of the lesion with respect to a healthy vessel. This means that severe stenosis may lead to larger uncertainties in the FFR values.

In this article, we analyze the effect of the pressure wire for different types of lesions both in realistic geometries and in an idealized vessel. For this purpose, we compare the FFRct values with invasive FFR in patients with wire versus values obtained without the pressure wire in CFD simulations. We then analyzed the influence of the pressure wire on an idealized vessel as a function of the diameter reduction and blood viscosity.

## 2. Methods

Two types of CFD simulations were performed; using an ideal cylindrical vessel with a constricted zone representing a stenosis, and coronary trees obtained from patients undergoing a FFR test and a computer tomography.

The ideal vessel consists of a cylinder of 3 mm [26,27] in diameter and 100 mm length. The stenosis has been simulated with an arc of circumference located at 50 mm and 2 mm from the center of the vessel, both for the long lesion (diffuse) and for the short lesion (acute), respectively. The pressure wire consists of a cylinder of 0.36 mm diameter (Philips Medical Systems) and a length of 4 mm. In the simulations, the wire is placed concentric to the vessel as shown in Fig. 1.

The influence of the wire on the FFR as a function of the cross-sectional diameter reduction $d/D$, where $D$ is the normal cross-sectional diameter and $d$ is the stenotic one, has been studied for long and short lesions. For $d/D > 85\%$, simulations approach total vessel occlusion, making the results unreliable. FFR was calculated 2 cm distal to the lesion [28]. A stenosis reduction has also been simulated where the area occupied by the pressure wire has been replaced by an equivalent stenosis diameter. In this case, the cross-sectional area reduction ranges from 0.72 % to 91 %.

For clinic simulations, 45 patients have been selected who have previously undergone the FFR test and a coronary computed tomography angiography (coronary CT). The coronary tree was reconstructed from the CT images using the 3DSlicer software [29]. The location of the pressure wire mimicked the invasive procedure [30]. The wire starts at the ostium and moves down the vessel to approximately 2–3 cm distal to the lesion [31] where the FFR is measured. 3DSlicer software was also used to place the wire. Blood flow simulations were performed using the StarCCM+ computational fluid dynamics (CFD) software, using the Navier-Stokes equations as the governing equations [32].

Simulations were conducted in a steady-state regime. The fluid was assumed to be incompressible and laminar, with a constant density of 1060 $kg/m^3$. For the patient-specific simulations, a constant viscosity of 0.004 Pa s was used [33,34]. However, for the ideal vessel study, a range of viscosity values was considered, spanning from 0.001 to 0.008 Pa s [35]. Additionally, non-Newtonian fluid simulations were conducted using the Carreau-Yassuda model [33] to investigate the impact of non-linear viscosity behavior on the flow characteristics (Table 1).

To solve the governing equations of the flow, a polyhedrical mesh that divides the 3D geometry into small subdomains was used and a

**Table 1**
Rheological parameters for the Carreau-Yasuda model [33].

| | |
|---|---|
| $n$ | 0.22 |
| $a$ | 1.25 |
| $\eta_0$ (Pa.s) | 5,60 $10^{-2}$ |
| $\eta_\infty$ (Pa.s) | 3,450$^{-3}$ |
| $\lambda$ | 1.902 |

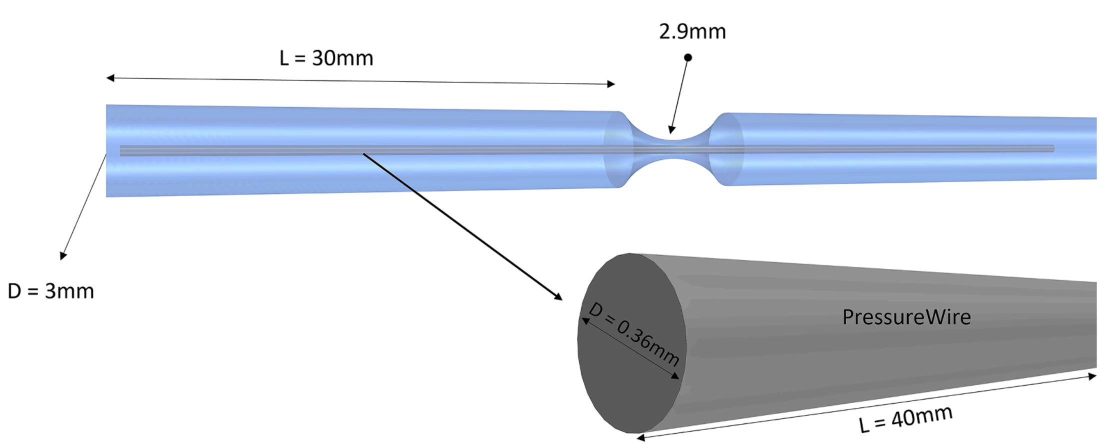


**Fig. 1.** Schematic of an idealized vessel.

mesh was considered in the coronary arteries and a coarse refinement in the aorta to reduce the computational cost without altering results. The meshes contain approximately 2 million faces without the pressure wire and 3.5 million when the wire is included. The exact number of elements can change depending on the characteristics of the 3D geometry. For this purpose, a mesh study was carried out for each geometry as in Otero-Cacho et al. [32]. For both models, a polyhedric mesh (Fig. 2) with a refinement of hexahedral elements near the wall and the pressure wire was used.

For both models, real and ideal vessel, a non-slip condition at the vessel rigid walls and the pressure wire was considered. Under steady state conditions, the mean arterial pressure ($P_m$) defined as the average pressure over the cardiac cycle is used as inlet condition and it is calculated based on the patient's own data obtained in a non-invasive way,

$$P_m = \frac{1}{3}P_s + \frac{2}{3}P_d \tag{1}$$

with $P_s$ and $P_d$ are the systolic and diastolic blood pressures, respectively. For each branch outlet, lumped (0D) boundary conditions were specified at the outlet of each artery. Hence, the branch resistance is calculated as $R = P_m/q$ (Pa s/m$^3$) and the estimation of the mean flow rate $\bar{q}$ follows van der Giessen et al. [36]. For the 45 patients, the flow $\bar{q}$ (m$^3$/s) and outlet diameter $D$ were fitted to the equation,

$$q = kD^x \tag{2}$$

by a non-linear regression analysis being $k = 1$ (m$^2$/s) and $x = 2{,}28$ for the real case [32]. For the ideal vessel we keep the same parameters to compare results. Finally, an implicit algorithm was used to calculate the outlet pressure $P$ (Pa) for each instant $t$,

$$P_{t+1} = (1-\alpha)P_t + \alpha R Q_t \tag{3}$$

where $\alpha$ is a relaxation parameter, and $Q_t$ ($m^3$/s) is the flow rate.

## 3. Results

In clinical patients and the idealized geometry, the impact of a pressure wire on the FFR computation has been investigated and contrasted with invasive FFR where available. Two types of lesions, elongated and acute, were considered for the ideal vessel. Furthermore, the question of whether a lesion with an equivalent area can replace the obstruction in the lesion caused by the pressure wire has been investigated. Lastly, an analysis was conducted for the idealized artery regarding the impact of blood viscosity on the FFR measurement.

### 3.1. Clinical patients

To evaluate the effect of a pressure wire on patients, simulations were performed on 45 volunteers with a total of 58 lesions, and the obtained results were compared with an invasive FFR. To that end, the three dimensional geometry was obtained from medical image segmentation and the FFRct was calculated using the CFD model as shown in Fig. 3.

Among the 58 lesions, 11 (19 %) were diagnosed with obstructive coronary artery disease. The FFRct results depended on the presence of the pressure wire. When employing the pressure wire, 10 patients exhibited a positive FFR (FFR<0.8); however, only 4 patients showed these results in the absence of the pressure wire. When analyzing the distribution of values within the grey zone (0,75−0,80), it is observed that there are 7 and 5 lesions for the FFRct cases with and without pressure wire, respectively, as compared to 5 lesions in the case of invasive FFR. Fig. 4 shows a resume of the relative error between FFR and FFRct calculated with and without the pressure wire. The results show that when the pressure wire is not employed, FFRct outcomes for individuals with FFR scores smaller than 0.8 are worse. The pressure wire's presence significantly alters the flow on severe lesions, which has an impact on the FFR calculation. In contrast, the impact of the pressure wire appears to be reduced when the FFR is larger than 0.8. Incorporating the wire in the simulations significantly enhances the accuracy of both negative and positive FFRct values and, thus, should be considered in the calculations.

The Bland-Altman analysis for both methods is shown in Fig. 5. Correlations between FFRct calculated with and without the pressure wire are shown in panels (a-b). Note that the statistical analysis revealed a strong correlation of [$r = 0{,}76,\ p < 0{,}001$] between FFRct with the pressure wire and invasive FFR measurements. In contrast, the correlation was slightly lower, but still significant [$r = 0{,}61,\ p < 0{,}001$] for the FFRct without the pressure wire, and an appreciable bias is observed mainly for small values of the FFR. These results are confirmed with the Bland-Altman plots (c-d). A negative trend is evident in the model without pressure wire with increasing FFR. However, with the introduction of the wire, this trend seems to have disappeared. Last plots demonstrated a slight difference but non-significant as compared with FFR in assessing the functional significance of stenosis.

To better comprehend the impact of the pressure wire on the overall accuracy of FFRct, we explore the relationship between simulations and invasive measurements. To discern the effect more clearly, we excluded any outliers from the patients sample. These outliers may have been caused by CT image artifacts, possibly resulting from the automated reconstruction performed by the CT scanner, subtly altering the vessel caliber at specific points within the coronary tree. Although such phenomena are relatively rare, our technique is highly sensitive to their influence. The introduction of a pressure wire leads to a non-linear perturbation in the FFR measurement, dependent on the luminal diameter of the artery. If this phenomenon can be accurately reproduced, a linear relationship should be observed between the pressure wire based simulations and the experimental data. To observe this, attention was directed towards the slope of the regression line, which allowed for a comparison between the model and the invasive data. For the pressure wire model, the slope demonstrated a noteworthy increase to 0.88, indicating a closer alignment between both methods. In

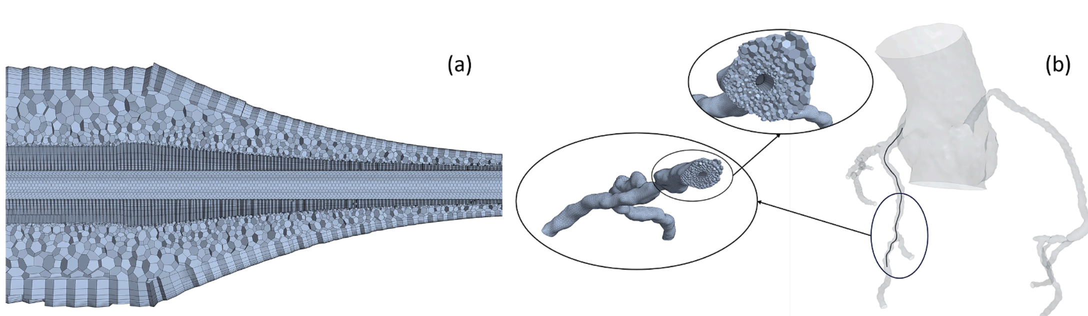


**Fig. 2.** CFD mesh used in the idealized vessel (a) and in a real patient (b). Note the mesh refinement near the walls and the pressure wire.

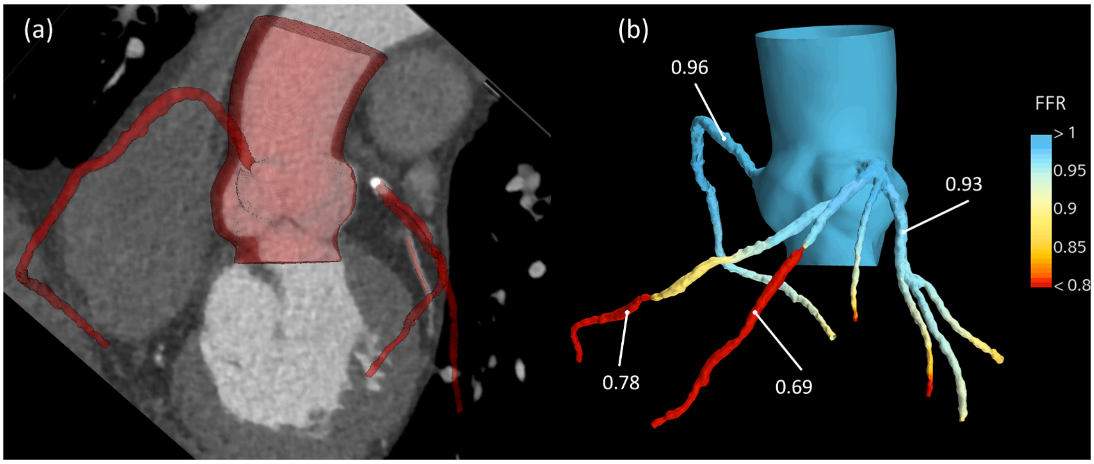


**Fig. 3.** (a) Medical image segmentation from which the 3D geometry of the patient is obtained. (b) FFRct calculated for that geometry for the whole coronary tree.

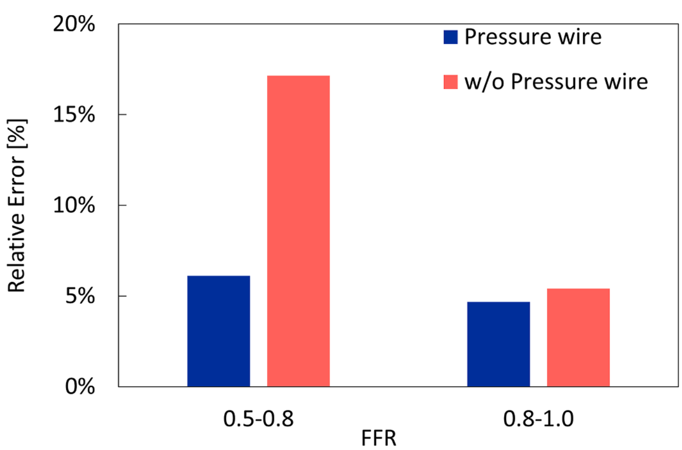


**Fig. 4.** Relative error $FFRct/FFR - 1$ with and without the pressure wire as a function of the invasive FFR.

contrast, without the pressure wire, the slope decreased to 0.46. Ideally, in the absence of experimental measurement variability and image segmentation uncertainties, the slope should approach the diagonal.

### 3.2. Ideal vessel

To better understand the influence of a pressure wire on coronary vessels, simulations were performed on an ideal geometry, enabling precise control over the size and type of stenosis. A focal lesion with two configurations, a small and an elongated lesion, was selected for the study. The impact of the pressure wire was investigated with respect to the severity of the stenosis for both cases. Fig. 6 shows the influence of the wire on flow rate within the vessels. Due to the obstruction caused by the wire and constant inlet pressure, the blood flow is reduced. This alteration in flow rate is reflected in the corresponding FFR values and it is more pronounced for the elongated lesions.

Fig. 7(a) shows the FFR values calculated for the elongated stenosis as a function of the occlusion percentage with and without considering the pressure wire. Similar results, not shown here, were obtained for the acute injury. Note that for severe occlusion ratios, the pressure drop becomes significant, above 60 % stenosis for the elongated lesion and 70 % for the small lesions. Panel (b) shows the FFR difference between both types of lesions. The pressure drop is more significant for the elongated lesion, primarily attributed to the flow acceleration through the stenosis for a longer duration, leading to the higher pressure drop, which can also be measured in terms of the wall shear stress. Larger differences were observed for significant stenosis (50 %−80 %) in both cases.

In clinical practice, a direct measurement of coronary flow is not feasible, and indirect measurements needs to be obtained. The flow rate calculated after the stenosis linearly correlates to the FFR as it has also been observed in Pijls et al. [11]. Around 70 % stenosis, the reduction in blood flow becomes significant, and in the most severe case of 85 % stenosis, the flow decreases by half compared to the healthy artery. When considering the pressure wire, the flow reduction becomes even more abrupt. The same 50 % flow reduction occurs at the 78 % stenosis level. The elongated lesion causes a larger reduction in flow compared to the short lesion. As both measurements are obtained under hyperemic conditions, a positive correlation is observed between the flow rate and FFR. Therefore, our data suggest that the type of lesion may be an important factor to consider for the coronary ischemia evaluation.

The influence of blood viscosity on the FFR values in the presence of a pressure wire is shown in Fig. 8. The non-Newtonian behaviour of the blood was studied using the Carreau-Yasuda model (Table 1). Significant differences were observed for stenosis occlusions above 60 % as described earlier. As expected, pressure drops after the stenosis (FFR decreases) with increasing flow viscosity and it is more pronounced as the percentage of occlusion increases. It is worth noting that the non-Newtonian model shows minimal disparities when compared to the model with constant viscosity (0.004 Pa.s). This is encouraging as it reinforces the confidence in the results presented throughout this article. Furthermore, adopting a model with constant viscosity optimizes computational efficiency [37].

The effect of a pressure wire in patient arteries has been compared to that in an idealized artery. To enhance visualization, data were averaged every 3 patients, sorted by the ratio between the pressure wire diameter and the lesion diameter. The difference in FFRs computed with and without the pressure wire as a function of the ratio of pressure wire and stenosis diameters is shown in Fig. 9. Note that the FFRct from patients follows a similar trend to that obtained from the idealized artery simulation. This suggests that the simplified model of the idealized artery could be useful to study real coronary vessels. The presence of the pressure wire on the flow is not limited to obstructing the stenosis but also modifies the flow around it. To that end, we simulated the vessel with an equivalent obstruction, but without the pressure wire (solid line). The dashed line in Fig. 9 shows that wall shear stresses caused by the presence of the wire are important to determine a correct FFR value, above all for severe stenosis.

Rather, it is the obstruction caused by the pressure wire relative to the stenosis diameter that is associated with the increasing pressure drop, independently of the patient's specific FFR value. Consequently, greater attention should be given to lesions where the pressure wire diameter to stenosis diameter ratio exceeds 30 %. Beyond this threshold,

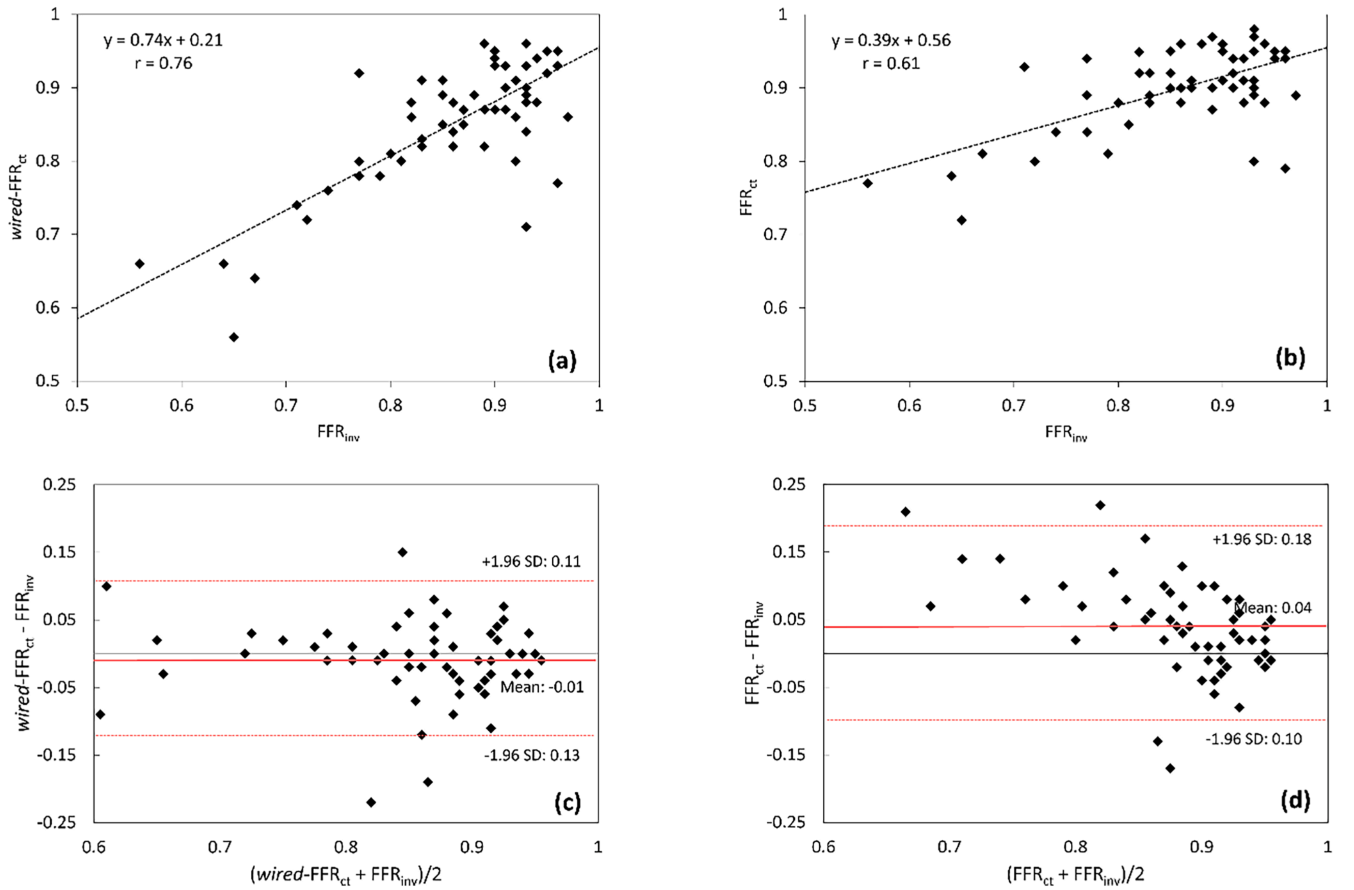


**Fig. 5.** Correlations between the pressure wire based FFRct (a) and the FFRct (b) as a function of the invasive FFR. Bland-Altman plots with (c) and without (d) pressure-wire-based FFRct.

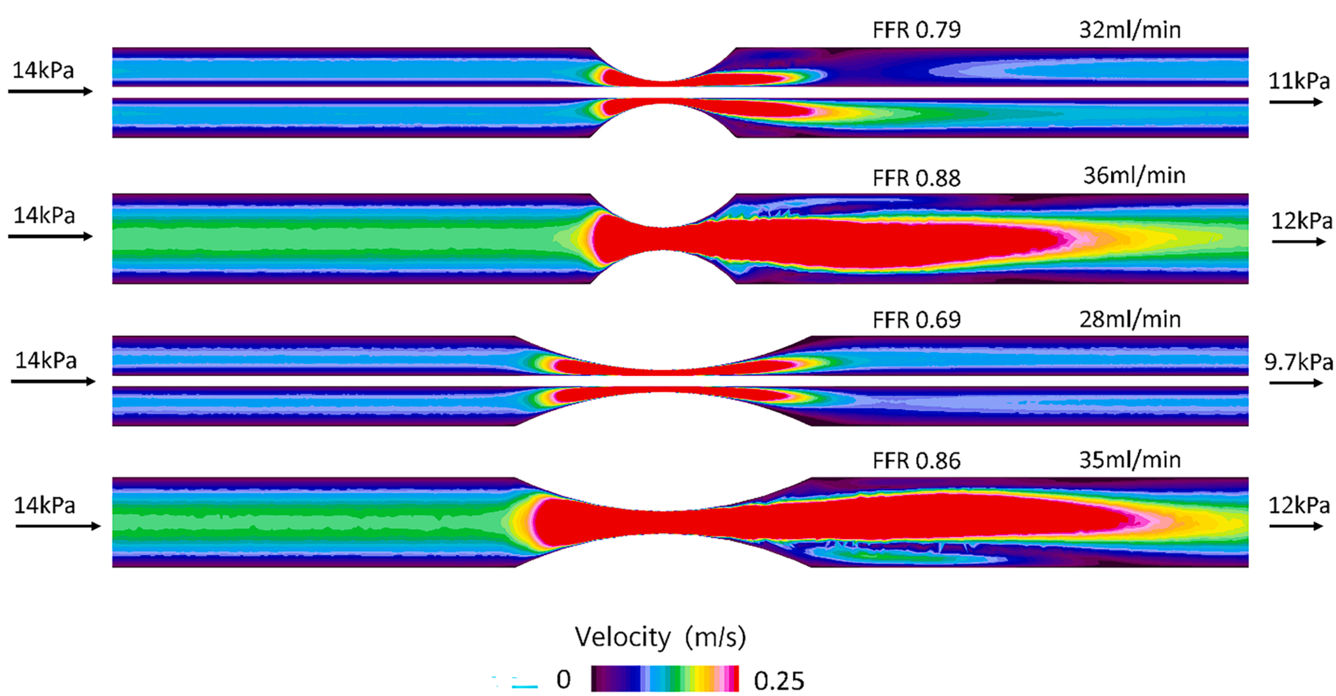


**Fig. 6.** Flow velocity for an ideal vessel with short and long stenosis cases with and without considering the pressure wire. In all cases, the inlet pressure was the same, 14 kPa. Note the smaller FFR values when considering the wire (white rectangle centered in two panels) that is more pronounced for the elongated lesion.

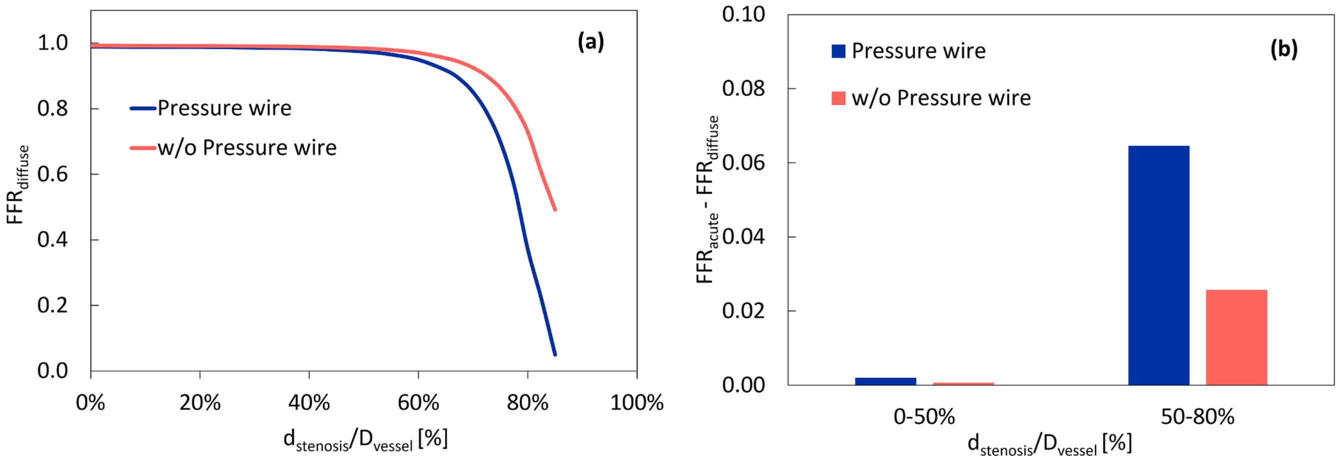


**Fig. 7.** (a) FFR as a function of the stenosis occlusion for an elongated injury considering or not the presence of a pressure wire. (b) Difference of FFR calculated for the short and elongated lesions.

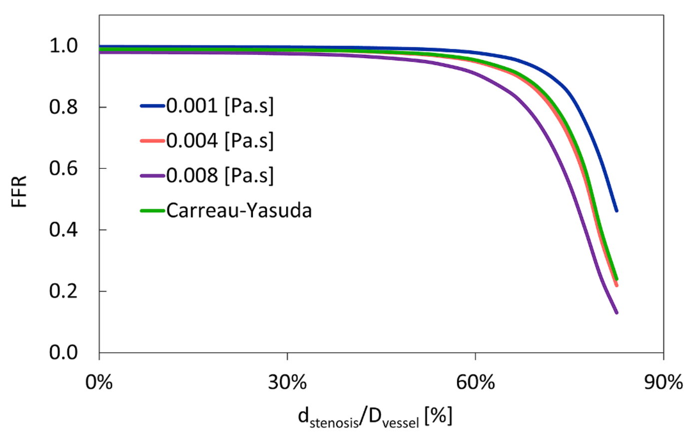


**Fig. 8.** FFR as a function of the elongated stenosis occlusion percentage considering a pressure wire and four blood viscosity values.

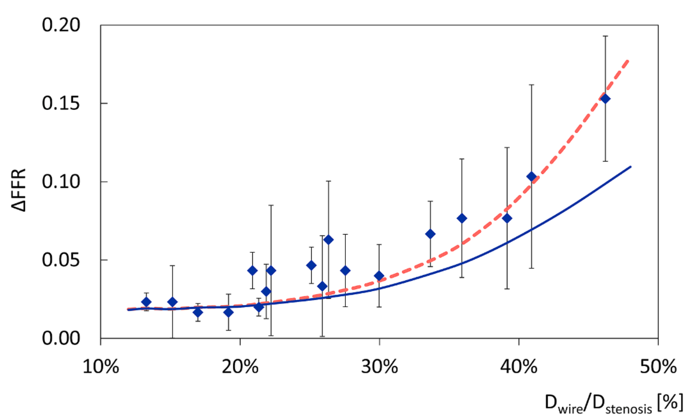


**Fig. 9.** Difference in FFRs computed with and without the pressure wire as a function of the ratio of pressure wire and stenosis diameters. Dashed line corresponds to CFD simulations using the pressure wire, while the solid line is for a vessel with an equivalent occlusion and no wire. Filled circles mark experimental FFR data as measured in the patient's lesions.

the obstruction caused by the pressure wire in the flow increases exponentially. Such cases could lead to classifying a lesion with a negative FFR as positive, above all near the threshold value of 0.8, where the highest uncertainty exists. The knowledge of the stenosis diameter enables us to ascertain whether the lesion is truly as severe as indicated by the FFR value. This information enables a more precise evaluation of multiple lesions with similar FFR values, underscoring the clinical significance of considering the relationship between pressure wire diameter and stenosis diameter accurately assessing FFR for coronary artery disease diagnosis.

## 4. Discussion

Here, we studied the influence of pressure wires on the measurement of Fractional Flow Reserve (FFR) through a combination of Computational Fluid Dynamics (CFD) simulations using 45 clinical patient data with 58 lesions and ideal geometries. Our results shed light on the implications of pressure wires in FFR measurements and provide valuable insights for clinical practice and the improvement of FFRct models [38]. The impact of pressure wires on FFR values is a crucial consideration for physicians when interpreting the significance of coronary stenosis [39–41]. While FFR cutoff values have been established to account for this influence [11], not much information is known on the specific effects of pressure wires, in particular, when their sizes become comparable to the lesions analyzed. Prior research has hinted at possible consequences connected to wires [42], but none have quantified these effects or explored their implications across the entire FFR spectrum in patients. Our results align with the work of Gould et al. [43] who demonstrated that stenosis with a lumen diameter reduction of 50 % or more lead to reduced hyperemic flow and increased coronary pressure drop. Consistent with their observations, we identified that the placement of wires during FFR measurements results in partial obstruction of the coronary artery lumen, leading to increased pressure drop and subsequent reduction in blood flow. Our analysis revealed that the most significant differences in FFR values were observed for severe stenosis, rather than only in cases with low FFR values. This suggests that the severity of low FFR values associated with severe stenosis may be prone to overestimation when compared to stenosis without severe narrowing. This observation holds practical implications, particularly in the interpretation of lesions falling within the "gray zone"(0,75 – 0,80).

Our results diverge from a recent study by Yi et al. [41], which concluded that the overestimation of FFR values in severe cases is of minor clinical importance since these critical lesions do not need sophisticated measurements. However, our study clearly demonstrates that the influence of pressure wires specifically affects severe stenosis with a lumen diameter reduction of 50 % or greater, irrespective of real or idealized geometries. This discrepancy highlights the need for further investigation and validation to reconcile these contrasting conclusions.

In addition to highlight the impact of the pressure guidewire on FFR as a function of stenosis diameter and illustrate how the effect of the pressure guidewire is exponential as it occupies a larger volume relative to the lesion, we explain that this result is not only due to the obstruction caused by the reduction of the stenosis area. To demonstrate this, we examine the flow behavior of a cross-section decrease without and with a guidewire. Our ideal simulation results agree with those obtained in real patients, making the findings on FFR behavior in the context of severe stenosis assessed with a pressure wire more relevant.

On other hand, we also investigate the effect of viscosity on stenosis. Our aim is to gain a solid understanding of the behaviour of variables relevant to clinical practice, such as viscosity and the influence of the pressure wire, which have not been studied deeply in the literature.

It is also worth noting that the sample of patients we present (45 patients) is much more significant than that used in other studies [44].

Moreover, our study has implications beyond clinical interpretation. We observed that incorporating the simulated presence of a wire during FFRct computation significantly improved the correlation between computed and invasive techniques. Accurately modelling the influence of wires poses a challenge due to the non-linear behaviour they induce in each vessel. Consequently, reproducing the entire phenomenon is necessary to capture the complex interaction between the wire and FFR measurements. This insight contributes to enhance the accuracy and reliability of FFRct models, offering potential advancements in non-invasive evaluation of coronary stenosis.

### *4.1. Limitations*

In this study the pressure guide is assumed to be rigid, maintaining a static and concentric position within the vessel. However, in patient specific cases, the guide tends to deviate from its static position within the vessel, necessitating further studies to comprehensively understand the implications of this phenomenon. Furthermore, the assumption of arterial rigidity across all cases may introduce potential limitations in accurately measuring FFR, as highlighted by existing studies [45]. However, additional research is needed to increase our knowledge in this matter. Simulations were performed under steady-state conditions, primarily due to the computational time advantages [32]. Nevertheless, it is important to acknowledge that blood flow exhibits pulsatile behavior, fluctuating with each heartbeat. Consequently, the boundary conditions, which simulate the peripheral resistance of the arterial system, should ideally adapt to the dynamic flow conditions at each instant of time. In the present study, however, the boundary conditions remained constant. Thus, further investigations are needed to assess the impact of pulsatile flow on FFR measurements. Lastly, this study encompassed a set of 45 patients, with 10 individuals (22 % of the sample) exhibiting an FFR value below 0.80. While these findings provide valuable insights, future research with a larger patient population is essential to validate and reinforce the outcomes derived from this study.

## 5. Conclusion

Our study underscores the importance of considering the influence of pressure wires in FFR measurements. When the pressure wire is not employed, FFRct outcomes for individuals with FFR scores smaller than 0.8 are worse. The pressure wire's presence significantly alters the flow on severe lesions, which has an impact on the FFR calculation. In contrast, the impact of the pressure wire appears to be reduced when the FFR is larger than 0.8. Incorporating the wire in the simulations significantly enhances the accuracy of both negative and positive FFRct values.

The findings provide critical information for physicians, emphasizing the need for cautious interpretation of FFR values, particularly in severe stenosis. It also offers insights into improving the correlation between FFRct models and invasive measurements by incorporating the influence of pressure wires. Further research is warranted to validate the relationship between pressure wires and FFR measurements.

Acknowledging the limitations of the study, such as the inherent assumptions and simplifications associated with CFD simulations, we believe that our work contributes to the existing knowledge and highlights the significance of addressing the impact of pressure wires in FFR assessments. Future studies should strive to refine the modelling of pressure wires influence and explore additional factors that may affect FFR measurements although our contribution clearly states that the pressure guide effect needs to be addressed specially when the ratio between the dimensions of the wire and the stenosis exceeds 30 %.

## Ethical approval

Patients referred from the emergency hospital chest pain unit for ischemic heart disease screening were included, selecting for invasive study those with at least one coronary lesion larger than 50 % in the CT angiography. Patients with subocclusive disease, previously implanted stent in the interrogated coronary artery, or very severe calcification that impeded adequate CT interpretation were excluded.

The development of the project was carried out respecting the Declaration of Helsinki of the World Medical Association 1964 and ratifications of the following assemblies (Tokyo 75, Venice 83, Hong Kong 89, Somerset West 96, Scotland 00, Seoul 08 and Fortaleza 13) on ethical principles for medical research on human beings, RD 1090/2015, of December 24, on clinical trials, specifically the provisions of article 38 on good clinical practices, and the Convention on human rights and biomedicine), made in Oviedo on April 4, 1997 and successive updates.

Researchers participating in this study agreed that all clinical data collected from the study subjects will be separated from personal identification data in such a way as to ensure the anonymity of the patient; respecting the Personal Data Protection Law (Organic Law 15/1999, of December 13), RD 1720/2007 of December 21, which approves the Regulations for the development of Organic Law 15/1999, Law 41/2002, of November 14 (basic regulation of patient autonomy and rights and obligations in terms of information and clinical documentation), as well as Law 3/2001, of May 28, (regulator of informed consent and the clinical history of patients), Law 3/2005, of March 7, modifying Law 3/2001 and Decree 29/2009 of February 5, which regulates access to historical electronic clinical data.

The clinical data of the patients were collected in the Case Report Form (CRF) specific to the study. Each CRF was encrypted protecting the identity of the patient. Only the research team and the health authorities, who have a duty to maintain confidentiality, will have access to all the data collected for the study. Only information that cannot be identified may be transmitted to third parties. Once the study is finished, the data will be destroyed.

The treatment, communication, and transfer of data were done in accordance with the provisions of the General Data Protection Regulation (Regulation (EU) 2016/679 of the European Parliament and of the Council, of April 27, 2016). The data collected were used for the purposes of the research study described in the protocol and kept for the time necessary to achieve the objectives of the study and in accordance with applicable legislation.

Research Ethics Committee Santiago-Lugo has approved this study and has set the conditions for sharing the data used in its development. As this is a retrospective study of medical records and archived samples that does not deviate from routine clinical practice, the Ethics Committee considers that patient informed consent and fully anonymization of the data before being access are enough requirements to carry out the study.

## Procedure protocol

Coronary computer tomography angiography (CT) images were obtained with a one-beat 16-cm wide coverage and a 0.23 mm spatial resolution (Revolution CT, GE Healthcare, Milwaukee, WI, USA). Acquisition parameters and patient premedication were chosen following the Society of Cardiovascular Computed Tomography recommendations. Invasive FFR was measured according to standard practice. Analogous to the invasive FFR, FFRct ≤ 0,80 was considered positive. To eliminate possible biases, the results of the invasive FFR were unknown at the time of applying this new model to obtain the FFRct value.

## Funding

This research has been supported by the Xunta de Galicia (Grant No. 2021-PG036-1), Sociedad Española de Cardiología (SEC/FEC-INV-CLI 22/04), the Spanish Ministerio de Ciencia e Innovación (Grants No. PID2022-138322OB-I00, PID2022-141626NB-I00, MCIN/AEI/10.13039/501100011033), European Union Next Generation EU/PRTR (Grant No: DIN2020-011068) and Interreg VI-A Spain. All these programs are co-funded by ERDF (EU).

## CRediT authorship contribution statement

**Alberto Otero-Cacho:** Writing – review & editing, Writing – original draft, Validation, Supervision, Resources, Project administration, Methodology, Formal analysis, Conceptualization. **Manuel Insúa Villa:** Writing – original draft, Software, Methodology, Investigation, Data curation, Conceptualization. **Diego López-Otero:** Writing – review & editing, Validation, Methodology, Investigation, Conceptualization. **Brais Díaz-Fernández:** Validation, Data curation. **María Bastos-Fernández:** Resources, Data curation. **Vicente Pérez-Muñuzuri:** Writing – review & editing, Visualization, Supervision, Formal analysis. **Alberto P. Muñuzuri:** Writing – review & editing, Supervision, Resources, Methodology, Investigation, Conceptualization. **José Ramón González-Juanatey:** Writing – review & editing, Supervision, Conceptualization.

## Declaration of competing interest

All authors declare that they have no conflicts of interest.

## References

[1] V.L. Feigin, G.A. Roth, M. Naghavi, P. Parmar, R. Krishnamurthi, S. Chugh, G. A. Mensah, B. Norrving, I. Shiue, M. Ng, K. Estep, K. Cercy, C.J.L. Murray, M. H. Forouzanfar, Global Burden of Diseases, Global burden of stroke and risk factors in 188 countries, during 1990-2013: a systematic analysis for the Global Burden of Disease Study 2013, Lancet Neurol. 15 (9) (2016) 913–924, https://doi.org/10.1016/S1474-4422(16)30073-4.

[2] D. Mozaffarian, E.J. Benjamin, A.S. Go, D.K. Arnett, M.J. Blaha, M. Cushman, S. de Ferranti, J.P. Després, H.J. Fullerton, V.J. Howard, M.D. Huffman, S.E. Judd, B. M. Kissela, D.T. Lackland, J.H. Lichtman, L.D. Lisabeth, S. Liu, R.H. Mackey, D. B. Matchar, D.K. McGuire, American Heart Association Statistics Committee, Stroke Statistics Subcommittee, Heart disease and stroke statistics–2015 update: a report from the American Heart Association, Circulation 131 (4) (2015) e29–e322, https://doi.org/10.1161/CIR.0000000000000152.

[3] S.S. Dhawan, R.P.A. Nanjundappa, J.R. Branch, W.R. Taylor, A.A. Quyyumi, H. Jo, M.C. McDaniel, J. Suo, D. Giddens, H. Samady, Shear stress and plaque development, Expert. Rev. Cardiovasc. Ther. 8 (2010) 545–556, https://doi.org/10.1586/erc.10.28.

[4] H. Samady, A. Kumar, Fractional flow reserve, JACC Cardiovasc. Interv. 10 (2017) 1402–1404, https://doi.org/10.1016/j.jcin.2017.05.009.

[5] Lam F.M.C., Salicio E.R., Aleman ̃G.B., 2020. FFR-TC como herramienta ú til para la deteccio ́n de lesiones coronarias hemodin ́amicamente significativas. Revista de ecocardiografia pr ́actica y otras t ́ecnicas de imagen card ́iaca 3, 6–10. 10.37615/retic.v3n2a3.

[6] W.F. Fearon, J.W. Chambers, A.H. Seto, I.J. Sarembock, G. Raveendran, C. Sakarovitch, L. Yang, M. Desai, A. Jeremias, M.J. Price, ACIST-FFR study (assessment of catheter-based interrogation and standard techniques for fractional flow reserve measurement), Circ. Cardiovasc. Imaging 10 (2017), https://doi.org/10.1161/circinterventions.117.005905.

[7] B.L. Nørgaard, T.A. Fairbairn, R.D. Safian, M.G. Rabbat, B. Ko, J.M. Jensen, K. Nieman, K.M. Chinnaiyan, N.P. Sand, H. Matsuo, J. Leipsic, G. Raff, Coronary CT angiography-derived fractional flow reserve testing in patients with stable coronary artery disease: recommendations on interpretation and reporting, Radiol. Cardiothorac. Imaging 1 (2019) e190050, https://doi.org/10.1148/ryct.2019190050.

[8] N.H. Pijls, J.A. van Son, R.L. Kirkeeide, B.D. Bruyne, K.L. Gould, Experimental basis of determining maximum coronary, myocardial, and collateral blood flow by pressure measurements for assessing functional stenosis severity before and after percutaneous transluminal coronary angioplasty, Circulation 87 (1993) 1354–1367, https://doi.org/10.1161/01.cir.87.4.1354.

[9] J.E. Davies, S. Sen, H.M. Dehbi, R. Al-Lamee, R. Petraco, S.S. Nijjer, R. Bhindi, S. J. Lehman, D. Walters, J. Sapontis, L. Janssens, C.J. Vrints, A. Khashaba, M. Laine, E.V. Belle, F. Krackhardt, W. Bojara, O. Going, T. Härle, C. Indolfi, G. Niccoli, F. Ribichini, N. Tanaka, H. Yokoi, H. Takashima, Y. Kikuta, A. Erglis, H. Vinhas, P. C. Silva, S.B. Baptista, A. Alghamdi, F. Hellig, B.K. Koo, C.W. Nam, E.S. Shin, J. H. Doh, S. Brugaletta, E. Alegria-Barrero, M. Meuwissen, J.J. Piek, N. van Royen, M. Sezer, C.D. Mario, R.T. Gerber, I.S. Malik, A.S. Sharp, S. Talwar, K. Tang, H. Samady, J. Altman, A.H. Seto, J. Singh, A. Jeremias, H. Matsuo, R.K. Kharbanda, M.R. Patel, P. Serruys, J. Escaned, Use of the instantaneous wave-free ratio or fractional flow reserve in PCI, N. Engl. J. Med. 376 (2017) 1824–1834, https://doi.org/10.1056/nejmoa1700445.

[10] M. Götberg, E.H. Christiansen, I.J. Gudmundsdottir, L. Sandhall, M. Danielewicz, L. Jakobsen, S.E. Olsson, P. Ohagen, H. Olsson, E. Omerovic, F. Calais, P. Lindroos, M. Maeng, T. Todt, D. Venetsanos, S.K. James, A. Karegren, M. Nilsson, J. Carlsson, D. Hauer, J. Jensen, A.C. Karlsson, G. Panayi, D. Erlinge, O. Frobert, Instantaneous wave-free ratio versus fractional flow reserve to guide PCI, N. Eng. J. Med. 376 (2017) 1813–1823, https://doi.org/10.1056/nejmoa1616540.

[11] N.H. Pijls, W.F. Fearon, P.A. Tonino, U. Siebert, F. Ikeno, B. Bornschein, M. van't Veer, V. Klauss, G. Manoharan, T. Engstrøm, K.G. Oldroyd, P.N.V. Lee, P. A. MacCarthy, B.D. Bruyne, Fractional flow reserve versus angiography for guiding percutaneous coronary intervention in patients with multivessel coronary artery disease, J. Am. Coll. Cardiol. 56 (2010) 177–184, https://doi.org/10.1016/j.jacc.2010.04.012.

[12] P.A. Tonino, B.D. Bruyne, N.H. Pijls, U. Siebert, F. Ikeno, M. van `t Veer, V. Klauss, G. Manoharan, T. Engstrøm, K.G. Oldroyd, P.N.V. Lee, P.A. MacCarthy, W. F. Fearon, Fractional flow reserve versus angiography for guiding percutaneous coronary intervention, N. Eng. J. Med. 360 (2009) 213–224, https://doi.org/10.1056/nejmoa0807611.

[13] R.K. Banerjee, A.S. Roy, L.H. Back, M.R. Back, S.F. Khoury, R.W. Millard, Characterizing momentum change and viscous loss of a hemodynamic endpoint in assessment of coronary lesions, J. Biomech. 40 (2007) 652–662, https://doi.org/10.1016/j.jbiomech.2006.01.014.

[14] B.K. Koo, A. Erglis, J.H. Doh, D.V. Daniels, S. Jegere, H.S. Kim, A. Dunning, T. DeFrance, A. Lansky, J. Leipsic, J.K. Min, Diagnosis of ischemia-causing coronary stenoses by noninvasive fractional flow reserve computed from coronary computed tomographic angiograms, J. Am. Coll. Cardiol. 58 (2011), https://doi.org/10.1016/j.jacc.2011.06.066, 1989–1997.

[15] J.K. Min, D.S. Berman, M.J. Budoff, F.A. Jaffer, J. Leipsic, M.B. Leon, G.J. Mancini, L. Mauri, R.S. Schwartz, L.J. Shaw, Rationale and design of the defacto (determination of fractional flow reserve by anatomic computed tomographic angiography) study, J. Cardiovasc. Comput. Tomogr. 5 (2011) 301–309, https://doi.org/10.1016/j.jcct.2011.08.003.

[16] M. Renker, U.J. Schoepf, R. Wang, F.G. Meinel, J.D. Rier, R.R. Bayer, H. Möllmann, C.W. Hamm, D.H. Steinberg, S. Baumann, Comparison of diagnostic value of a novel noninvasive coronary computed tomography angiography method versus standard coronary angiography for assessing fractional flow reserve, Am. J. Cardiol. 114 (2014) 1303–1308, https://doi.org/10.1016/j.amjcard.2014.07.064.

[17] K. Tanaka, H.G. Bezerra, S. Gaur, G.F. Attizzani, H.E. Bøtker, M.A. Costa, C. Rogers, B.L. Nørgaard, Comparison between non-invasive (coronary computed tomography angiography derived) and invasive-fractional flow reserve in patients with serial stenoses within one coronary artery: a NXT trial substudy, Ann. Biomed. Eng. 44 (2015) 580–589, https://doi.org/10.1007/s10439-015-1436-y.

[18] T.P. van de Hoef, R. Petraco, M.A. van Lavieren, S. Nijjer, F. Nolte, S. Sen, M. Echavarria-Pinto, J.P. Henriques, K.T. Koch, J. Baan, R.J. de Winter, M. Siebes, J.A. Spaan, J.G. Tijssen, M. Meuwissen, J. Escaned, J.E. Davies, J.J. Piek, Basal stenosis resistance index derived from simultaneous pressure and flow velocity measurements, EuroIntervention 12 (2016) e199–e207, https://doi.org/10.4244/eijv12i2a33.

[19] A. Kumar, E.W. Thompson, A. Lefieux, D.S. Molony, E.L. Davis, N. Chand, S. Fournier, H.S. Lee, J. Suh, K. Sato, Y.A. Ko, D. Molloy, K. Chandran, H. Hosseini, S. Gupta, A. Milkas, B. Gogas, H.J. Chang, J.K. Min, W.F. Fearon, A. Veneziani, D. P. Giddens, S.B. King, B.D. Bruyne, H. Samady, High coronary shear stress in patients with coronary artery disease predicts myocardial infarction, J. Am. Coll. Cardiol. 72 (2018) 1926–1935, https://doi.org/10.1016/j.jacc.2018.07.075.

[20] R. Nakazato, H.B. Park, D.S. Berman, H. Gransar, B.K. Koo, A. Erglis, F.Y. Lin, A. M. Dunning, M.J. Budoff, J. Malpeso, J. Leipsic, J.K. Min, Noninvasive fractional flow reserve derived from computed tomography angiography for coronary lesions of intermediate stenosis severity, Circ. Cardiovasc. Imaging 6 (2013) 881–889, https://doi.org/10.1161/circimaging.113.000297.

[21] F.R. AL-Obaidi, W.F. Fearon, A.S. Yong, Invasive physiological indices to determine the functional significance of coronary stenosis, IJC Heart Vasc. 18 (2018) 39–45, https://doi.org/10.1016/j.ijcha.2018.02.003.

[22] A. Candreva, G.D. Nisco, M.L. Rizzini, F. D`Ascenzo, G.M.D. Ferrari, D. Gallo, U. Morbiducci, C. Chiastra, Current and future applications of computational fluid dynamics in coronary artery disease, Rev. Cardiovasc. Med. 23 (2022) 377, https://doi.org/10.31083/j.rcm2311377.

[23] V. Eslami, M. Safi, M. hasan Namazi, M. Pishgahi, A. Eftekharzade, S. A. Eftekharzadeh, Value of delta fractional flow reserve ({*upDelta*FFR) for predicting coronary ischemic lesions, Galen Med. J. 9 (2020) e1528, https://doi.org/10.31661/gmj.v9i0.1528.

[24] H.A. Himburg, D.M. Grzybowski, A.L. Hazel, J.A. LaMack, X.M. Li, M.H. Friedman, Spatial comparison between wall shear stress measures and porcine arterial

endothelial permeability, Am. J. Physiol. Heart Circ. Physiol. 286 (2004) H1916–H1922, https://doi.org/10.1152/ajpheart.00897.2003.
[25] H. Takagi, Y. Ishikawa, M. Orii, H. Ota, M. Niiyama, R. Tanaka, Y. Morino, K. Yoshioka, Optimized interpretation of fractional flow reserve derived from computed tomography: comparison of three interpretation methods, J. Cardiovasc. Comput. Tomogr. 13 (2019) 134–141, https://doi.org/10.1016/j.jcct.2018.10.027.
[26] I. Coma-Canella, A. Maceira, D. Dorronsoro, J. Calabuig, A. Martínez, Changes in the diameter of the coronary arteries in heart transplant recipients with angiographically normal vessels during five years, Rev. Esp. Cardiol. 52 (7) (1999) 485–492.
[27] A.K. Hiteshi, D. Li, Y. Gao, A. Chen, F. Flores, S.S. Mao, M.J. Budoff, Gender differences in coronary artery diameter are not related to body habitus or left ventricular mass, Clin. Cardiol. 37 (10) (2014) 605–609.
[28] S.H. Kueh, J. Mooney, M. Ohana, U. Kim, P. Blanke, R. Grover, S. Sellers, J. Ellis, D. Murphy, C. Hague, et al., Fractional flow reserve derived from coronary computed tomography angiography reclassification rate using value distal to lesion compared to lowest value, J. Cardiovasc. Comput. Tomogr. 11 (2017) 462–467.
[29] B. Serrano-Antón, A. Otero-Cacho, D. López-Otero, B. Díaz-Fernández, M. Bastos-Fernández, V. Pérez-Muñuzuri, J.R. González-Juanatey, A.P. Muñuzuri, Coronary artery segmentation based on transfer learning and unet architecture on computed tomography coronary angiography images, IEEe Access 11 (2023) 75484–75496, https://doi.org/10.1109/ACCESS.2023.3293090.
[30] Y. Abuouf, M. AlBadawi, S. Ookawara, M. Ahmed, Effect of guidewire insertion in fractional flow reserve procedure for real geometry using computational fluid dynamics, Biomed. Eng. 20 (2021), https://doi.org/10.1186/s12938-021-00935-y. Online.
[31] M. Matsumura, N.P. Johnson, W.F. Fearon, G.S. Mintz, G.W. Stone, K.G. Oldroyd, B.D. Bruyne, N.H. Pijls, A. Maehara, A. Jeremias, Accuracy of fractional flow reserve measurements in clinical practice, JACC Cardiovascular. Interv. 10 (2017) 1392–1401, https://doi.org/10.1016/j.jcin.2017.03.031.
[32] A. Otero-Cacho, D. López-Otero, M. Insúa Villa, B. Díaz-Fernández, M. Bastos-Fernández, V. Pérez-Muñuzuri, A. P Muñuzuri, J.R. González-Juanatey, Validation of a new model of non-invasive functional assessment of coronary lesions by computer tomography fractional flow reserve, REC CardioClinics (2023), https://doi.org/10.1016/j.rccl.2023.07.004.
[33] Y.I. Cho, K.R. Kensey, Effects of the non-newtonian viscosity of blood on flows in a diseased arterial vessel. part 1: steady flows, Biorheology 28 (1991) 241–262, https://doi.org/10.3233/bir-1991-283-415.
[34] J. Jung, D. Lee, K. Kim, M. Choi, Y. Cho, H. Lee, S. Choi, S. Lee, D. Kim, Reference intervals for whole blood viscosity using the analytical performance-evaluated scanning capillary tube viscometer, Clin. Biochem. 47 (2014) 489–493, https://doi.org/10.1016/j.clinbiochem.2014.01.021.
[35] E. Nader, S. Skinner, M. Romana, R. Fort, N. Lemonne, N. Guillot, A. Gauthier, S. Antoine-Jonville, C. Renoux, M.D. HardyDessources, E. Stauffer, P. Joly, Y. Bertrand, P. Connes, Blood rheology: key parameters, impact on blood flow, role in sickle cell disease and effects of exercise, Front. Physiol. 10 (2019), https://doi.org/10.3389/fphys.2019.01329.
[36] A.G. van der Giessen, H.C. Groen, P.A. Doriot, P.J. de Feyter, A.F. van der Steen, F. N. van de Vosse, J.J. Wentzel, F.J. Gijsen, The influence of boundary conditions on wall shear stress distribution in patients specific coronary trees, J. Biomech. 44 (2011) 1089–1095, https://doi.org/10.1016/j.jbiomech.2011.01.036.
[37] G. De Nisco, M. Lodi Rizzini, R. Verardi, C. Chiastra, A. Candreva, G. De Ferrari, F. D`Ascenzo, D. Gallo, U. Morbiducci, Modelling blood flow in coronary arteries: newtonian or shear-thinning non-newtonian rheology? Comput. Methods Programs Biomed. 242 (2023) 107823 https://doi.org/10.1016/j.cmpb.2023.107823.
[38] C.M. Cook, R. Petraco, M.J. Shun-Shin, Y. Ahmad, S. Nijjer, R. Al-Lamee, Y. Kikuta, Y. Shiono, J. Mayet, D.P. Francis, S. Sen, J.E. Davies, Diagnostic accuracy of computed tomography–derived fractional flow reserve, JAMa Cardiol. 2 (2017) 803, https://doi.org/10.1001/jamacardio.2017.1314.
[39] E. Cami, T. Tagami, G. Raff, T.A. Fonte, B. Renard, M.J. Gallagher, K. Chinnaiyan, A. Bilolikar, A. Fan, A. Hafeez, R.D. Safian, Assessment of lesion-specific ischemia using fractional flow reserve (FFR) profiles derived from coronary computed tomography angiography (FFRCT) and invasive pressure measurements (FFRINV): importance of the site of measurement and implications for patient referral for invasive coronary angiography and percutaneous coronary intervention, J. Cardiovasc. Comput. Tomogr. 12 (2018) 480–492, https://doi.org/10.1016/j.jcct.2018.09.003.
[40] R. Petraco, S. Sen, S. Nijjer, M. Echavarria-Pinto, J. Escaned, D.P. Francis, J. E. Davies, Fractional flow reserve–guided revascularization, JACC Cardiovasc. Interv. 6 (2013) 222–225, https://doi.org/10.1016/j.jcin.2012.10.014.
[41] J. Yi, F.B. Tian, A. Simmons, T. Barber, A computational analysis of the influence of a pressure wire in evaluating coronary stenosis, Fluids 6 (2021) 165, https://doi.org/10.3390/fluids6040165.
[42] J. Rodés-Cabau, M. Gutiérrez, J. Courtis, E. Larose, J.P. Déry, M. Coté, C. M. Nguyen, O. Gleeton, G. Proulx, L. Roy, B. NoÃl, G. Barbeau, R.D. Larochelli`ere, S. Rinfret, O.F. Bertrand, Importance of diffuse atherosclerosis in the functional evaluation of coronary stenosis in the proximal-mid segment of a coronary artery by myocardial fractional flow reserve measurements, Am. J. Cardiol. 108 (2011) 483–490, https://doi.org/10.1016/j.amjcard.2011.03.073.
[43] K. Gould, K. Lipscomb, G.W. Hamilton, Physiologic basis for assessing critical coronary stenosis, Am. J. Cardiol. 33 (1974) 87–94, https://doi.org/10.1016/0002-9149(74)90743-7.
[44] Z. Yan, Z. Yao, W. Guo, D. Shang, R. Chen, J. Liu, J. Ge, Impact of pressure wire on fractional flow reserve and hemodynamics of the coronary arteries: a computational and clinical study, IEEE Trans. Biomed. Eng. 70 (5) (2022) 1683–1691.
[45] A.S.C. Yong, A. Javadzadegan, W.F. Fearon, A. Moshfegh, J.K. Lau, S. Nicholls, M. K.C. Ng, L. Kritharides, The relationship between coronary artery distensibility and fractional flow reserve, PLoS One 12 (2017) e0181824, https://doi.org/10.1371/journal.pone.0181824.